J. Earth Syst. Sci. (2020)129 15
https://doi.org/10.1007/s12040-019-1266-7

The Palaeogene record of Himalayan erosion in the Andaman Basin

Neeraj Awasthi[1,2,*] and Jyotiranjan S Ray[1]

[1] *Geosciences Division, Physical Research Laboratory, Navrangpura, Ahmedabad 380 009, India.*
[2] *Present address: Department of Earth and Planetary Sciences, Prof. Rajendra Singh (Rajju Bhaiya) Institute of Physical Sciences and Research, VBS Purvanchal University, Jaunpur 222 003, India.*
**Corresponding author. e-mail: aneeraj.geology@gmail.com*

MS received 19 April 2019; revised 13 July 2019; accepted 16 July 2019

The Himalayan orogeny has been recognized as one of the most important Cenozoic events that shaped the geography, climate and ocean chemistry of our planet. The erosion in the Himalayas is believed to have played a critical role in crustal deformation and changes in the chemistry of the ocean water since the Eocene. In spite of the fact that the orogeny began after India–Asia collision at 59±1 Ma, the record of its earliest erosional history is meagre. In an attempt to fill this gap in the knowledge, we studied temporal changes in provenance of Paleogene–Neogene siliciclastic sediments of the Andaman Islands, deposited in a trench-forearc basin in the Bay of Bengal. Using Sr-isotope stratigraphy and tephrochronology we determined the timings of depositions of various lithologies. Sediment sources were identified using trace element and isotopic (Sr–Nd) fingerprinting. Results of our study suggest that the Myanmar Arc had remained a constant sediment source to the Andaman basin during 55–5 Ma, whereas the basin started receiving significant continental sands input after 35 Ma that increased with time until ∼20 Ma. Geochemical provenance of these sands suggests their derivation from Precambrian crustal sources in the Himalaya, which probably is an outcome of higher erosional rates subsequent to a rapid exhumation of the orogen in the late Eocene and efficient sediment transport through the palaeo-channels of the rivers Brahmaputra and Ganga under optimal conditions of the Indian monsoon. Such a scenario is consistent with the idea that the Himalayan sediment input is the cause for the conspicuous rise in marine $^{87}Sr/^{86}Sr$ since ∼40 Ma. Our data also suggest that since the Miocene, sediment sources in the Indo-Burman Ranges and the Myanmar arc have become the major contributors to the Andaman Basin through the Irrawaddy river system.

Keywords. Andaman Islands; provenance; tectonics; Himalaya; Sr–Nd isotopic ratios.

1. Introduction

The interaction between tectonics and climate is probably best manifested in the Cenozoic geological events in South Asia linked to the formation of the Himalayan mountain belt, which began ∼60 million years ago (Hu *et al.* 2016, 2017). It has been hypothesized that the rise of the Himalaya and the formation of the Tibetan Plateau had profound thermal and dynamic effects on the Asian climate (Molnar *et al.* 2010). The rise of the Himalaya and the surrounding mountain belts is generally attributed to multiple phases of thrusting and folding events following the closure of the

Supplementary material pertaining to this article is available on the *Journal of Earth System Science* website (http://www.ias.ac.in/Journals/Journal_of_Earth_System_Science).

Published online: 20 December 2019

Neo-Tethys (e.g., Jamieson *et al.* 2004). Whereas our understanding of the evolution of these geographical features and their role in the development or modulation of the climate remains poor, the influence of climate on them is well established by the fact that heavy precipitation caused by the South Asian monsoon system along these belts produces one of highest erosional fluxes contributing significantly to the chemical evolution of seawater since the Eocene (e.g., Palmer and Edmond 1992; Krishnaswami *et al.* 1992). This massive denudation believed to have also affected the Himalayan topography by altering the regional crustal thermal structure and stress field leading to isostatic rebound (e.g., Pinter and Brandon 1997). The weathering of silicate rocks in these mountain belts is believed to be a major factor in the drawdown of the atmospheric CO_2 which is responsible for global cooling in Cenozoic (e.g., Raymo and Ruddiman 1992; Edmond and Huh 1997). Quantification of the effects of weathering and erosional processes and their influence on the carbon cycle and regional/global climate requires a comprehensive understanding of the temporal evolution of these mountain belts, which is, in one way, come from the sedimentary records of the eroded material. Unfortunately, such direct records are rare within the orogen or immediate hinterland as the available records are mostly of the Neogene period and very limited of the Paleogene. Because of paucity of such sedimentary records, our understanding of the Himalayan orogeny during its early stages between ∼60 and ∼20 Ma, is poor.

This study is an attempt to bring to light some of the unknowns of the Himalayan orogeny and its erosional history during the Late Eocene to Oligocene by studying the sedimentary sequences deposited in the Andaman trench to forearc basin of the Bay of Bengal that are currently exposed in the Andaman Accretionary Prism (AAP). The reasons for selecting these rocks are that they were believed to have been deposited during the early-middle Cenozoic (Bandopadhyay and Carter 2017) and contain abundant siliciclastic turbidites derived from the surrounding continents, and hence likely to preserve records of the eroded material from the Himalaya mountain belt, particularly from its extension in the east. We carried out a comprehensive geological and geochemical study of these sediments with the objective to reconstruct the time series of erosion and weathering in the Himalaya and South Asian landmasses, and to trace the depositional pathways through time and understand their implications for the paleodrainage and paleoclimate in the region. Building on earlier studies and using $^{87}Sr/^{86}Sr$-stratigraphic ages and tephrochronology, we establish stratigraphy of sedimentation and determine secular changes in sediment provenance using trace elements, and Nd–Sr isotopic compositions of siliciclastic sediments.

2. Geology of Andaman Islands

The archipelago of the Andaman and Nicobar Islands is part of an accretionary complex located on the outer arc ridge of the Sunda–Andaman subduction zone, at which the Indian plate subducts obliquely beneath the Burmese (Myanmar) microplate – a sliver of the Eurasian plate (Curray 2005; McCaffrey 2009), along the Andaman Trench (figure 1A). The Indo-Burman Ranges (IBR) in Myanmar represents the northward extension of this accretionary complex. The Andaman Sea to its east is an active extensional basin that encompasses the forearc and backarc basins of the subduction zone (Curray 2005), separated by an island arc ridge containing two subaerial volcanoes (figure 1A). The Andaman Islands expose segments of oceanic lithosphere, pelagic sediments and turbidites through an imbricate stack of east-dipping thrust slices and folds (Pal *et al.* 2003; Bandopadhyay and Ghosh 2015).

Lithologically, the sedimentary succession exposed on the Andaman–Nicobar Islands can be broadly classified into the five major groups: the Ophiolite Group, the Mithakhari Group, the Andaman Flysch Group, the Archipelago Group and the Nicobar Group as shown in figure 2(A) (Curray 2005). All groups, except the Andaman Flysch, are bounded by well-developed unconformities (figure 2A). The Ophiolite Group that occurs at the bottom of the sequence contains ocean floor volcanic/plutonic rocks and pelagic sediments at the top (figure 2A). These plutonic rocks are of upper Cretaceous age (∼94 Ma; Pedersen *et al.* 2010; Srinivasa Sarma *et al.* 2010; figure 2). The Ophiolite Group is overlain by the Mithakhari Group of Eocene period (>40 Ma; Allen *et al.* 2007), with the latter consisting of trench-slope deposits of conglomerate, sandstone, shale and volcaniclastics (figure 2A and C). The Oligocene–Early Miocene Andaman Flysch Group (∼30–20 Ma; Allen *et al.* 2007) contains submarine fan deposits comprising largely unfossiliferous siliciclastic turbidites in the form of sandstone-shale rhythmites (figure 2A and D; Bandopadhyay and

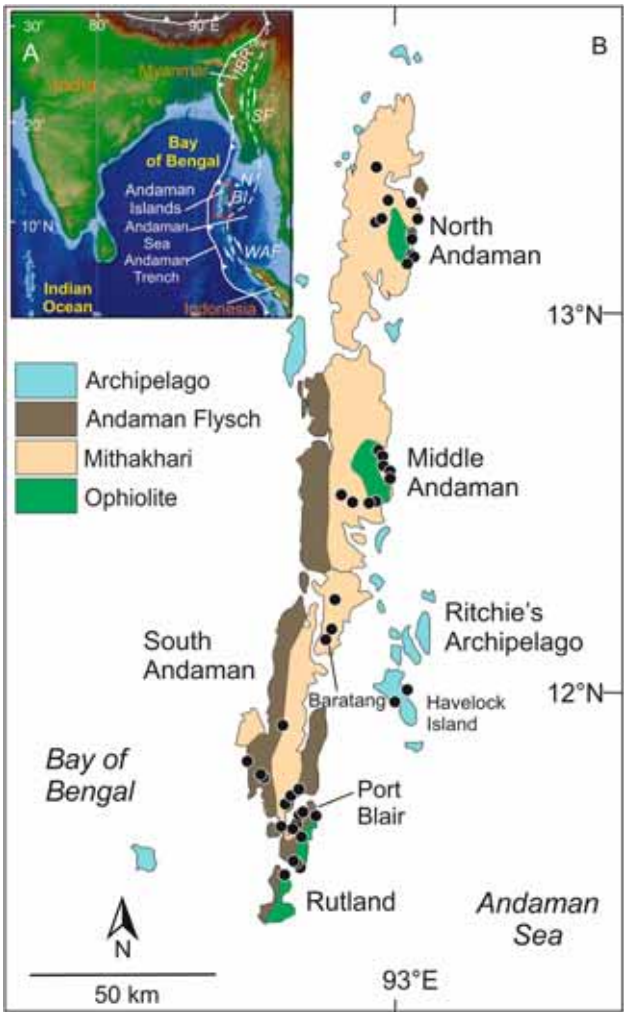

Figure 1. **(A)** Map of the northeastern Indian Ocean showing various tectonic and geomorphic features of the Sunda–Andaman Subduction Zone and its northward extension. Barren Island (BI) and Narcondam (N) are volcanic islands of the Andaman Arc. SF: Sagaing Fault; WAF: West Andaman Fault; IBR: Indo-Burman Ranges. **(B)** A blow-up of the boxed area showing a detailed geological map of the Andaman Islands with the sample locations marked as dots. The Nicobar Group is not mapable on the scale presented, hence not shown.

Ghosh 2015). The Mio-Pliocene Archipelago Group rocks comprised mostly of carbonate rocks with minor siliciclastics and volcaniclastic sediments and are believed to have been deposited in a marine shelf environment (figure 2A and E; Bandopadhyay and Ghosh 2015). The topmost Nicobar group contains limestones, beach deposits, unclassified volcanic rocks and tuffs of Pleistocene age. The existing biostratigraphic and chronological data suggest that the bulk of the siliciclastics of the AAP was deposited sometime during the Paleogene and early Neogene, although the durations of various groups, particularly the top two, remain tentative.

Earlier studies on provenance of sediments in the AAP had limited spatiotemporal coverage, confined to the stratigraphic units of the Mithakhari and Andaman Flysch Groups of Port Blair area, South Andaman (Allen *et al.* 2007; Bandopadhyay and Ghosh 2015). Although the work of Allen *et al.* (2007) had the benefit of a few ^{40}Ar–^{39}Ar and U–Pb age data for detrital minerals and Nd isotopic data for the Andaman Flysch Group, it lacked trace element and Sr isotopic data for the entire succession. Allen *et al.* (2007) had suggested that the sediments in the Mithakhari Group were predominantly derived from the magmatic arc located in Myanmar and had a subordinate contribution from the continental margin located to the east of the arc. According to them, the sediments of Andaman Flysch Group were derived from recycled orogen sources in Myanmar (e.g., Shan-Thai Terrane; Mogok Metamorphic Belt) with minor arc-derived material. The work of Bandopadhyay and Ghosh (2015) on geochemistry of the Andaman Flysch Group rocks also had similar inferences. In a recent work based on integrated sandstone petrography, heavy minerals, and U–Pb ages of detrital zircons from the group, Limonta *et al.* (2017) suggested that the Andaman Flysch turbidites have a provenance similar to the Himalayan-derived sediments of the Paleogene Bengal Fan (Najman *et al.* 2008) and they received very little contribution from the Myanmar sources. Although all studies recognized that part of sedimentary record in the AAP might represent off scraped portions of early Bengal fan, they have either ruled out any significant contributions from the nascent Himalaya and/or Indian cratonic sources or fallen short of categorically suggesting the same. Interestingly though, some Paleogene and most Neogene successions of the IBR, an extension of the AAP to the north, contain sediments derived from the Himalayan sources (Allen *et al.* 2008).

3. Materials and methods

The samples studied in this work were collected from different sedimentary units, including carbonates and volcaniclastics, from all the five groups on the Andaman Islands (figures 1B and 2A). Details of sampling information with locations are provided in table 2 of Awasthi (2017). Efforts were made to collect least altered samples and have a large spatial coverage with equal representation from various sectors. Geochemical and isotopic

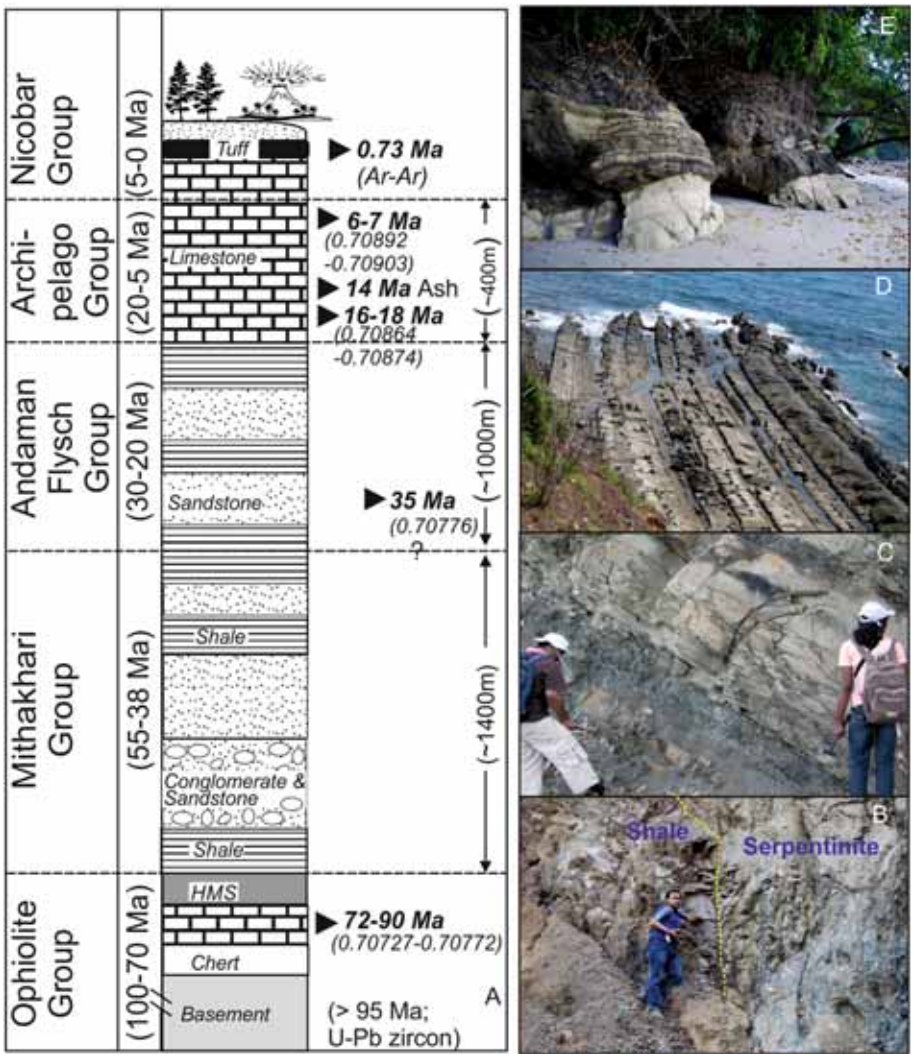

Figure 2. **(A)** Stratigraphic litholog showing broad lithological variations on the Andaman Islands prepared based on literature (e.g., Curray 2005; Pal *et al.* 2003) and inferences from our own field investigations. Ages in brackets on the left are approximate depositional age ranges from Allen *et al.* (2007) and Curray (2005). U–Pb zircon age for ophiolite basement is from Pedersen *et al.* (2010). Ages given on the right of the litholog are obtained from Sr isotope stratigraphy ($^{87}Sr/^{86}Sr$ values are in brackets) of carbonate formations (this work), tephrochronology in Archipelago Group using isotope fingerprinting (this work) and ^{40}Ar–^{39}Ar dating of the Mile Tilek Tuff, Nicobar Group (Awasthi *et al.* 2015). HMS = hemipelagic mudstone. **(B–E)** Field photographs of the Ophiolitic basement, a sandstone outcrop of the Mithakhari Group, quartz wacke-shale turbidites (Bouma sequences) of the Andaman Flysch Group, and carbonate turbidites of the Archipelago Group, respectively.

analyses were performed on selected whole-rock samples. Handpicked chips were powdered and homogenized. Silicate rock samples were decarbonated using 2N HCl and their organic matter was removed by combustion at 600°C before they were processed for geochemical and isotopic analyses. Silicate fractions of the limestones were extracted as residues after 6N HCl leaching of whole rock powders. Silicate samples/fractions were dissolved using conventional HF–HNO_3 protocol and final stock solutions were prepared in 2% HNO_3 for elemental analyses. Trace element concentrations were measured using a quadrupole inductively coupled plasma mass spectrometer (Q-ICPMS) at Physical Research Laboratory, Ahmedabad following the procedure described in Awasthi (2017). International rock standard BHVO-2 was used as a calibration standard as well as an unknown for accuracy and precision checks.

Sr and Nd isotopic ratios of siliciclastic sediments were determined following the standard HF–HNO_3–HCl rock dissolution and Sr–Nd preconcentration techniques using cation exchange column chemistry (Awasthi *et al.* 2014). Carbonate rocks studied for Sr-isotope stratigraphy were dissolved in ultra-pure acetic acid and Sr was

separated using Sr-specific resin following the protocol of Ray *et al.* (2003). Sr–Nd isotopic ratio measurements were carried out on an Isoprobe-T TIMS. Sr and Nd isotope ratios were corrected for fractionation using $^{86}Sr/^{88}Sr = 0.1194$ and $^{146}Nd/^{144}Nd = 0.7219$, respectively. The average values for NIST SRM 987 Sr and JNdi-1 Nd standards analyzed over a period of 4 yrs, respectively were $^{87}Sr/^{86}Sr = 0.710234 \pm 0.000008$ and $^{143}Nd/^{144}Nd = 0.512104 \pm 0.000004$ ($\pm$ 0.1 in ε_{Nd} units) at the 2σ level of uncertainty. The value of $^{143}Nd/^{144}Nd = 0.512104$ for JNdi-1 corresponds to a value of 0.511847 for the widely used La Jolla Nd standard (Awasthi *et al.* 2014). For comparison with data from the literature, all the $^{87}Sr/^{86}Sr$ data for the siliciclastic sediments were normalized to a value of 0.71025 for NBS987 and $^{143}Nd/^{144}Nd$ to a value of 0.511858 for La Jolla. All plots and discussion below are based on the normalized ratios. All analytical data utilized in this study are presented in table 1. We define ε_{Nd} or $\varepsilon_{Nd}(0) = \{((^{143}Nd/^{144}Nd)_S - (^{143}Nd/^{144}Nd)_{CHUR})/(^{143}Nd/^{144}Nd)_{CHUR}\} \times 10^4$ where subscript 'S' stands for sample and 'CHUR' stands for Chondrite Uniform Reservoir, and Nd-model age $T_{DM} = (1/\lambda) \times \{1 + ((^{143}Nd/^{144}Nd)_S - (^{143}Nd/^{144}Nd)_{DM})/((^{147}Sm/^{144}Nd)_S - (^{147}Sm/^{144}Nd)_{DM})\}$ where subscript 'DM' stands for depleted mantle. Other details are given in the footnote of table 1.

4. Results and discussion

4.1 *Chronology*

The ranges of $^{87}Sr/^{86}Sr$ for least altered carbonate samples from limestone formations are presented alongside the stratigraphic column in figure 2(A). Using principles of Sr-isotope stratigraphy of McArthur *et al.* (2012) we dated the pelagic carbonate units of the Ophiolite Group, occurring at the upper part of the sequence, from 72–90 Ma (figure 2A). Likewise, carbonate leached from a shale sample belonging to the Andaman Flysch Group (figure 1B; figure 2) gave an age of 35 Ma. The Sr–isotope stratigraphic age of the bottommost limestone formation of the Archipelago group in the Havelock Island (figure 1B) was determined to be 16–18 Ma, whereas that of the siliceous limestone formation of the same group in the Baratang Island, Middle Andaman (figure 1B) yielded ages in the range of 6–7 Ma (figure 2). The limestone in the Havelock Island contains a significant amount of volcaniclastic component. The Sr–Nd isotopic compositions of this component (table 1) closely resemble the dacitic and rhyolitic ejecta of the 14 Ma eruptions in the Wuntho-Popa volcanic arc of Myanmar (Lee *et al.* 2016), which was then located closer to the Andaman basin. We therefore infer that the tephra bearing limestones of the Havelock Island are ~14 Ma old. Considering the results of Sr-isotope stratigraphy and tephrochronology, it can be concluded that the deposition of the Archipelago Group limestones in Havelock occurred during 18–14 million years ago. Using these new depositional ages and existing information, we establish a robust stratigraphy for the AAP (figure 3A), in which the timings of the Ophiolite–Mithakhari and Mithakhari–Andaman Flysch transitions are placed at ~55 and ~35 Ma, respectively. Based on field evidence we came to a conclusion that the boundary between the Mithakhari and Andaman Flysch groups is gradational (figure 3A). This inference is primarily based on the observation that there is no apparent break in sedimentation between the two groups of rocks as the topmost coarse-grained sandstone of the Mithakhari Group smoothly grades into the bottommost cross-bedded sandstone of the Andaman Flysch Group.

4.2 *Provenance of sediments*

The stratigraphic variations of the geochemical and isotopic data, for 46 siliciclastic samples, are plotted in figure 3. For the sake of completeness, the data for volcaniclastic sediments, present either as silicate fractions in limestones or independent tuff layers, are also plotted (vol in figure 3). As expected, they show predominantly magmatic compositions ($^{87}Sr/^{86}Sr = 0.704489$–$0.709157$; $\varepsilon_{Nd} = -1.9$ to $+2.9$; $T_{DM} = 0.45$ to 0.83 Ga) akin to Cenozoic volcanic ejecta from the Andaman–Indonesian magmatic arc (Awasthi *et al.* 2015). The red hematitic mudstone formation at the top of the Ophiolite Group (figure 2A), has $^{87}Sr/^{86}Sr > 0.71$, $\varepsilon_{Nd} < -1.4$ and $T_{DM} > 1.0$ Ga, which indicate incorporation of minor continental (terrigenous) sediments that usually contain highly radiogenic Sr ($^{87}Sr/^{86}Sr > 0.72$) and non-radiogenic Nd ($\varepsilon_{Nd} < -10$). An examination of the post-Gondwana paleogeographic reconstructions (Hall 2012; Boonchaisuk *et al.* 2013; Replumaz *et al.* 2014) suggests that the likely provenances of the terrigenous components of the mudstone could have been the west Burma block or the Sibumasu (Shan-Thai) block of Myanmar, when the Greater

Table 1. *Geochemical and isotopic compositions of Andaman Island siliciclastic sediments.*

Sample	$^{87}Sr/^{86}Sr$	$^{143}Nd/^{144}Nd$	$\varepsilon_{Nd}(0)$	T_{DM}	Th	Nb	La	Sr	Nd	Zr	Sm	Eu	Gd	Yb	Sc
Nicobar Group (Mile Tilak Tuff: 0.73 Ma)															
AND-11-54G	0.709157	0.512606	–0.6	0.83	9.7	3	26	969	22	52	4.7	1.1	4.66	2.1	3.8
AND-11-54W	0.707246	0.512683	+0.9	0.58	11.9	4	21	487	14	73	2.5	0.7	2.31	1.6	5.9
Archipelago Group (silicate fraction)															
Baratang Limestone (6–7 Ma)															
AND-09-07	0.718673	0.511990	–12.6	1.54	7.4	6	14	94	12	25	2.2	0.5	1.98	1.0	5.4
AND-09-08	0.720602	0.511936	–13.7												
Havelock Island Tuffaceous Limestone (14 Ma)															
AND-09-64	0.705606	0.512539	–1.9												
AND-09-65	0.705166	0.512602	–0.7												
AND-09-66	0.704489	0.512786	+2.9	0.45	6.2	4	16	170	13	113	2.4	0.7	2.43	1.6	6.4
Andaman Flysch Group															
PB-08-07	0.720311	0.512163	–9.3	1.40	11.8	11	37	74	36	17	7.0	1.5	6.10	1.3	11.6
PB-08-09	0.721051	0.512007	–12.3	1.49	31.2	14	68	105	62	27	11.1	1.8	8.91	2.3	12.7
AND-09-04	0.715480	0.512142	–9.7	1.51	10.6	9	30	78	29	22	6.0	1.3	5.45	1.5	6.3
AND-09-12	0.730491	0.511987	–12.7	1.62	12.4	8	26	17	25	27	4.8	1.0	4.11	1.1	1.6
AND-09-36	0.718371	0.512157	–9.4	1.47	7.6	7	23	73	22	21	4.6	1.1	4.11	1.2	6.2
AND-09-42	0.721361	0.512085	–10.8	1.62	9.0	6	30	53	24	12	4.9	1.0	4.06	0.8	7.6
AND-09-43	0.716050	0.512059	–11.3	1.51	14.4	10	43	77	34	40	6.5	1.4	5.51	1.3	13.6
AND-09-61	0.725155	0.512091	–10.7												
AND-09-61A	0.723225	0.512089	–10.7	1.75	9.9	9	38	67	40	31	8.8	2.0	7.73	2.1	6.9
AND-11-6a	0.716945	0.512066	–11.2	1.55	11.1	9	34	153	31	20	6.2	1.3	5.94	1.7	9.0
AND-11-22	0.728232	0.512004	–12.4	1.47	19.9	7	48	81	41	37	7.3	1.1	6.04	1.4	11.1
AND-11-23	0.729019	0.512033	–11.8	1.56	10.1	8	27	91	25	8	4.7	1.0	4.10	1.0	8.5
Collinpur	0.723954	0.512050	–11.5	1.35	23.7	10	66	93	47	8	7.9	1.2	6.86	1.6	8.5
Mithakhari Group															
PB-08-08	0.710924	0.512237	–7.8	1.26	10.9	8	30	115	26	16	5.0	1.1	4.40	1.0	11.1
PB-08-11	0.711301	0.512278	–7.0												
PB-08-12	0.706312	0.512222	–8.1												
PB-08-13	0.706567	0.512604	–0.7	0.86	3.8	4	14	75	15	32	3.3	1.0	3.35	1.4	5.8

AND-09-02	0.706566	0.512851	+4.2	0.69	2.6	2	34	194	57	65	15.4	4.6	16.13	6.7	24.9
AND-09-03	0.710017	0.512344	–5.7	1.12	8.6	6	26	70	24	16	4.6	1.0	4.09	1.1	5.4
AND-09-05	0.711100	0.512316	–6.3	1.23	7.5	7	23	115	23	9	4.6	1.1	4.21	0.9	11.1
AND-09-06	0.706655	0.512708	+1.4	0.69	5.5	3	16	53	17	24	3.7	1.0	3.60	1.4	8.6
AND-09-10	0.706929	0.512502	–2.7	1.03	5.6	3	16	134	17	24	3.7	1.0	3.62	1.4	6.1
AND-09-14	0.715538	0.512473	–3.2	0.80	7.1	7	21	27	19	59	3.1	0.7	2.75	1.5	7.1
AND-09-19	0.708003	0.512500	–2.7	1.85	3.1	4	12	41	19	24	5.4	1.6	5.73	1.7	10.2
AND-09-20	0.705513	0.512835	+3.8	0.62	2.1	4	11	137	15	61	3.7	1.5	4.05	2.4	16.1
AND-09-22	0.706831	0.512823	+3.6	0.57	2.3	4	12	35	17	61	3.9	1.3	4.20	2.0	14.8
AND-09-24	0.707492	0.512551	–1.7	1.01	3.3	4	19	127	19	26	4.2	1.2	4.57	1.7	6.9
AND-09-26	0.706721	0.512784	+2.8												
AND-09-27	0.711964	0.512630	–0.2	0.68	7.1	7	23	37	17	68	3.2	0.6	3.05	1.8	6.6
AND-09-28	0.706725	0.512728	+1.8												
AND-09-30	0.705757	0.512729	+1.8	0.81	5.1	6	17	154	23	145	5.7	1.5	6.11	3.4	20.4
AND-09-33	0.706576	0.512630	–0.2												
AND-09-37	0.707029	0.512510	–2.5	1.06	3.1	4	15	102	15	18	3.4	1.0	3.60	1.0	4.4
AND-09-44	0.709516	0.512547	–1.8	1.05	5.9	6	19	56	23	45	5.3	1.3	5.27	1.7	10.9
AND-09-52	0.708561	0.512667	+0.6												
AND-09-54	0.704972	0.512833	+3.8	0.63	2.5	4	11	152	15	74	3.9	1.4	4.26	2.8	18.3
AND-09-55	0.705544	0.512796	+3.1	0.68	1.7	3	10	101	13	43	3.2	1.1	3.42	1.9	17.3
Ophiolite Group (Pelagic sediments)															
AND-09-48	0.710206	0.512371	–5.2	1.30	6.4	10	18	92	22	66	4.9	1.2	4.62	1.5	13.0
AND-09-49	0.712552	0.512564	–1.4	0.95	6.0	7	15	41	19	86	4.2	1.1	4.18	2.2	17.9
BHVO-2 (m)	0.70345	0.512949			1.2	16	15	360	25	150	6.2	2.1	6.40	2.0	29
BHVO-2 (*r*)	0.70344$^{\$}$	0.512957$^{\$}$			1.2$^{\#}$	16$^{\#}$	15$^{\#}$	382$^{\#}$	24$^{\#}$	160$^{\#}$	6.0$^{\#}$	2.0$^{\#}$	6.20$^{\#}$	2.0$^{\#}$	31$^{\#}$

Note: Sr, Nd isotopic data are given as ratios whereas trace elements concentrations are given in 'ppm' and T_{DM} (Nd-model age) in Ga. $\varepsilon_{Nd(0)} = \{[(^{143}Nd/^{144}Nd)_S - (^{143}Nd/^{144}Nd)_{CHUR}]/(^{143}Nd/^{144}Nd)_{CHUR}\}\times 10^4$ where subscript 'S' stands for sample and 'CHUR' stands for Chondrite Uniform Reservoir. The present day $^{143}Nd/^{144}Nd$ value of CHUR is 0.512638. $T_{DM} = 1/\lambda\{1+[(^{143}Nd/^{144}Nd)_S - (^{143}Nd/^{144}Nd)_{DM}]/[(^{147}Sm/^{144}Nd)_S - (^{147}Sm/^{144}Nd)_{DM}]\}$ where subscripts 'DM' stands for depleted mantle, $(^{143}Nd/^{144}Nd)_{DM} = 0.513114$ and $(^{147}Sm/^{144}Nd)_{DM} = 0.222$ (Michard *et al.* 1985). The last two rows present measured (m) and reported (*r*) values of isotopic ratios in USGS rock standard BHVO-2 (n=13), analyzed as an unknown. Reproducibility of trace element contents, based on the repeated analyses of the BHVO-2 standard, were ≤5% for REEs and ≤10% for all other trace elements at 2σ level. $ = data of Raczek *et al.* (2003), # = data of Kent *et al.* (2004).

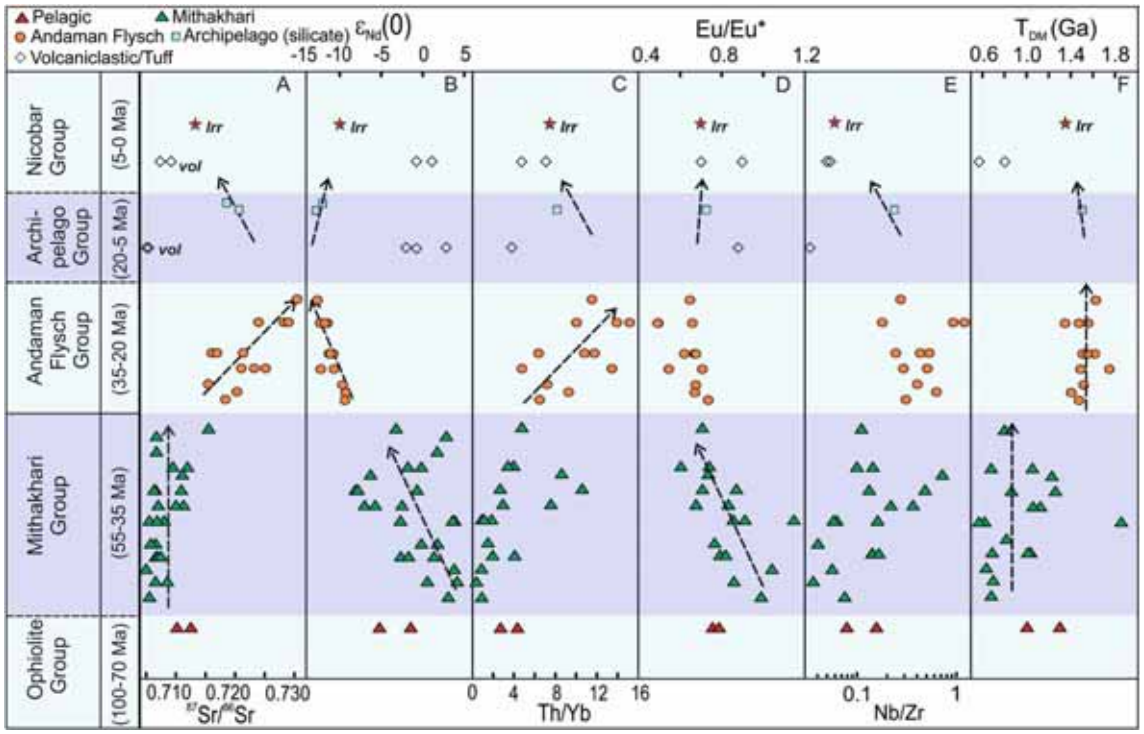

Figure 3. Stratigraphic variations of various geochemical and isotopic proxies in siliciclastics and silicate fractions in limestones are presented in (**A**–**F**); data for which are given in table 1. Data for volcaniclastic sediments in tuffs and limestones are also presented. Isotopic compositions of modern sediment in Irrawaddy River (Irr) are marked (data source: Colin *et al.* 1999). Arrows show the secular trends in the data. Vol is volcaniclastic and T_{DM} represents the Nd-model age of derivation from a depleted mantle. Approximate depositional ages in brackets on the left are modified ages based on the present work.

Indian subcontinent was located below 10°S, far from the subduction front, ∼70 million years ago.

The siliciclastics of the Mithakhari Group, representing the trench-slope sediments, possess highly variable trace element contents and Sr–Nd isotopic ratios (table 1), and lack clear stratigraphic trends (figure 3). Their less radiogenic $^{87}Sr/^{86}Sr$ (0.708 ± 0.003), high ε_{Nd} (range: –8.1 to +4.2; average: –1.0 ± 4.0), low T_{DM} (0.9 ± 0.3 Ga), low Nb/Zr (0.18 ± 0.19), low Th/Yb (3.5 ± 2.9) and high Eu/Eu* (0.8 ± 0.1) point to a dominant contribution from juvenile (mantle) source component. The range of ε_{Nd} composition as reported by Allen *et al.* (2007) falls well within the range observed by us. The prominent negative anomalies of Nb and Ta, and enriched large ion lithophile element (LILE) patterns in most of these samples suggest that this juvenile component was derived predominantly from a magmatic arc and not from the basement ophiolite (figure 4). However, considering that conglomerate horizon of the Mithakhari Group contains clasts of mafic and ultramafic igneous rocks (figure 2A), we cannot completely rule out the ophiolite basement of the AAP as a local sediment source in some parts of the basin. Interestingly, high $^{87}Sr/^{86}Sr$ (>0.710), low ε_{Nd} (<–5) and high Th/Sc (>1.0) observed in a few samples (table 1) hint at the presence of a subordinate continent-derived component. In ε_{Nd} *vs.* $^{87}Sr/^{86}Sr$ plot (figure 5A), more than 40% of the samples show compositions similar to that of the volcanic arc of Myanmar and the rest plot well within the fields of Trans-Himalayan and Sibumasu rocks, which have continental crustal affinity. This could mean that either each of these three sources dominated the sediment budget of the basin at different times/spaces or the sediments represent variable mixtures of materials derived from the Myanmar arc and one of the other two sources (figure 5A). Further statistical scrutiny of the Nd isotopic composition of these sediments and their probable sources using Kernel Density Estimation (KDE; figure 5B) also supports the inferences drawn from figure 5(A), as the density function for ε_{Nd} of the sediments lacked clear peaks. Other isotopic and trace elemental ratio cross plots for the Mithakhari samples also suggest sediment sourcing from volcanic arc and continental (upper) crustal sources, examples being the Andaman arc and old crustal rocks from Himalaya, respectively (figures 6 and 7). Because the rocks of the Sibumasu block are compositionally similar to

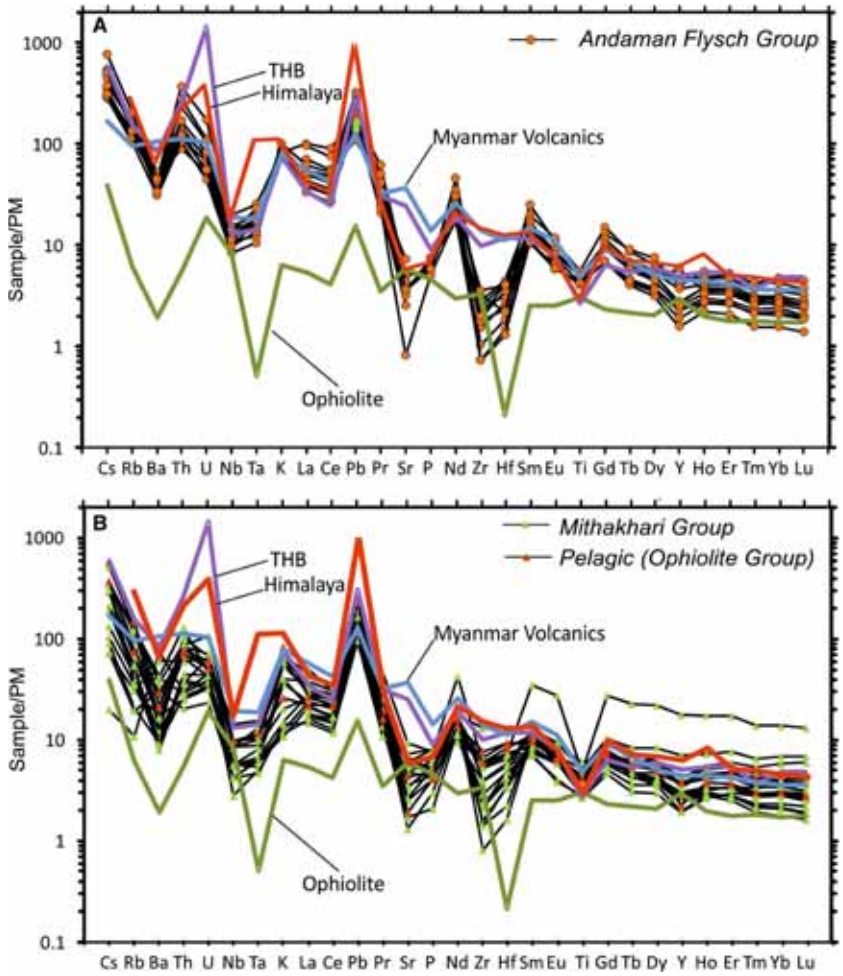

Figure 4. Primitive mantle (PM) normalized trace element patterns for siliciclastic formations of the (A) Andaman Flysch Group (B) Mithakhari and Ophiolite Groups. A complete trace element data for the studied samples is given in Awasthi (2017). For comparison, average compositions of probable sources are also shown (see data in table S1 of supplementary file). THB is Trans-Himalyan Batholith sources.

those of the Trans-Himalayas, it is quite likely that most of the Mithakhari sediments, including the arc-derived detritus, came from the west Burma block. However, there exists a finite probability that the rocks of the Trans-Himalaya could have contributed to the Andaman basin during the Eocene as they did to the Assam Basin to the north (Vadlamani *et al.* 2015).

Unlike the Mithakhari Group rocks, the finer grained and quartz-bearing sediments of the Andaman Flysch Group show systematic variations with time in most geochemical proxies of provenance (figure 3). From ∼35 through ∼20 Ma, sediment input to the Andaman Basin became increasingly radiogenic in Sr ($^{87}Sr/^{86}Sr$ = 0.71548–0.73049) and non-radiogenic in Nd ($\varepsilon_{Nd}(0)$ = –9.4 to –12.7), which indicate increasing continental input (figure 3). Further support for this inference comes from the finding of secular increase in quartz content (Pal *et al.* 2003), increasing Th/Yb, and decreasing Eu/Eu* (figure 3). Dominance of continental input is highlighted by the trace element patterns (figure 4A) and other geochemical parameters such as $f^{Sm/Nd}$, ε_{Nd} and Th/Sc ratios (figures 6 and 7). The earlier reported whole-rock $\varepsilon_{Nd}(0)$ values (–11.2 and –8.2; Allen *et al.* 2007) are well within the range observed by us. In ε_{Nd} *vs.* $^{87}Sr/^{86}Sr$ plot, the Andaman Flysch sediments fall in the fields defined for the Trans-Himalayan, Sibumasu and Higher Himalayan rocks, similar to the sediments in the Barail Group of the Bengal Basin (figure 5A). Because a clear Himalayan provenance has been identified for the Eocene–Oligocene Barail sediments (Najman *et al.* 2008), we envisage the same for the Andaman Flysch. The KDE peak for these rocks, although overlap with that for Sibumasu and Trans-Himalayan sources, has certainly some influence of

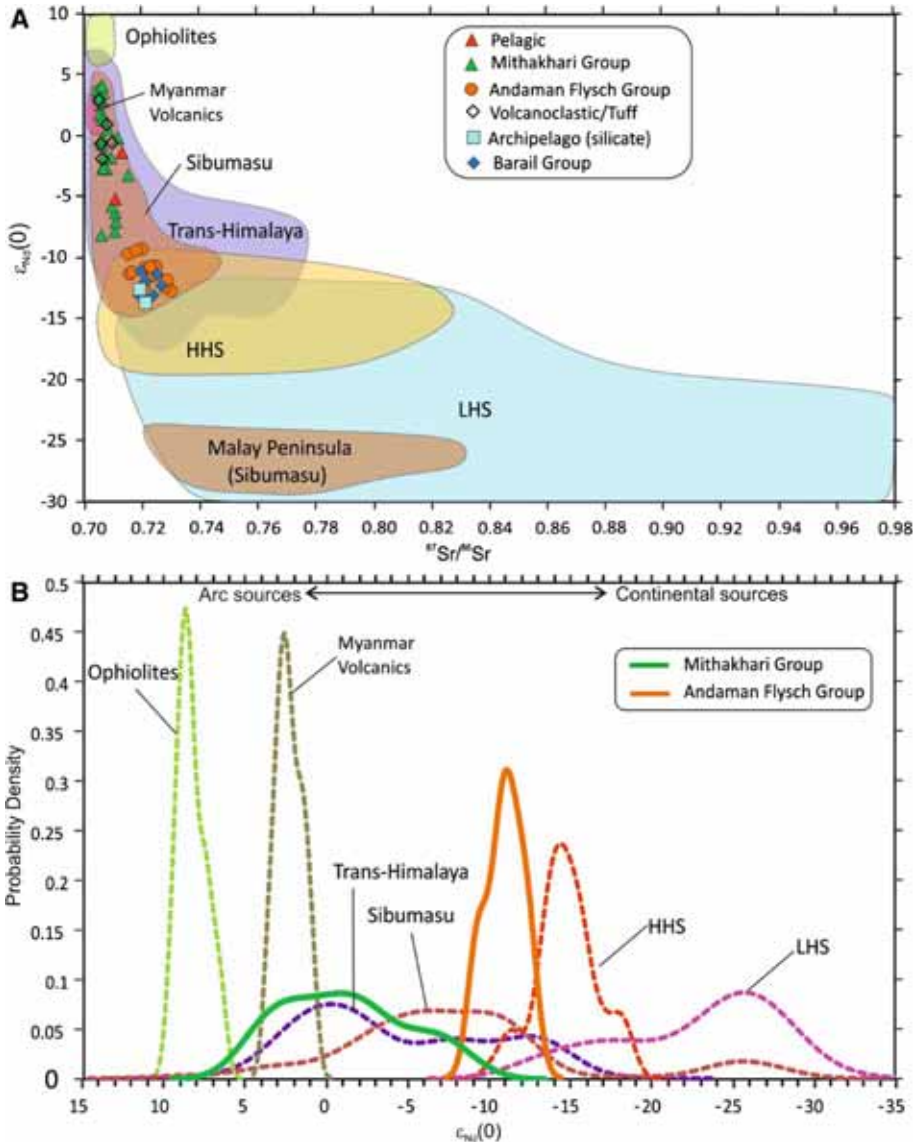

Figure 5. **(A)** $^{87}Sr/^{86}Sr$ *vs.* $\varepsilon_{Nd}(0)$ plot for the siliciclastic sediments of the Andaman Accretionary Prism along with data for the Paleogene Barail Group sediments (Bengal Basin) and fields for the potential sediment sources. Data Sources: Barail Group – Hossain *et al.* (2010), Bracciali *et al.* (2015); Myanmar Volcanics – Lee *et al.* (2016); Himalaya (LHS, HHS) – Awasthi *et al.* (2018). For Trans-Himalayan and Sibumasu sources data see table S2 of supplementary file. **(B)** Kernel Density Estimate (KDE) plot showing probability density function for ε_{Nd} of Andaman sediments compared with that of various probable sediment sources. HHS: Higher Himalayan Sources, LHS: Lesser Himalayan Sources.

sources in the Higher Himalaya (figure 5B). Other isotopic and trace element plots (figures 4 and 6) clearly suggest that the sediments of the Andaman Flysch were primarily derived from continental sources, likely from Precambrian upper crustal rocks. The Proterozoic Nd-model ages of these sediments (T_{DM} = 1.40–1.75 Ga; figure 3F) also support this inference.

The continental input to the Andaman Flysch could have had three potential sources that could have contributed either exclusively or collectively: the eastern India craton (Singhbhum craton and its north-eastern extension), the rising Himalayan orogen and the Sibumasu block. The first could not have been a major source as it would have introduced sediments with very high non-radiogenic Nd ($\varepsilon_{Nd} < -25$; Sharma *et al.* 1994; Saha *et al.* 2004; Rashid *et al.* 2018) into the basin, which apparently is not the case (figure 3B). Also, it is difficult to imagine large quantities of sediment supply from these continental sources because the Bengal Basin (or fan) that was situated in-between is not known to have received much sediment from these sources after the Eocene (Najman *et al.* 2008; Hossain *et al.* 2010; Roy and Roser 2013). The west Burma block cannot be considered as a major continental source

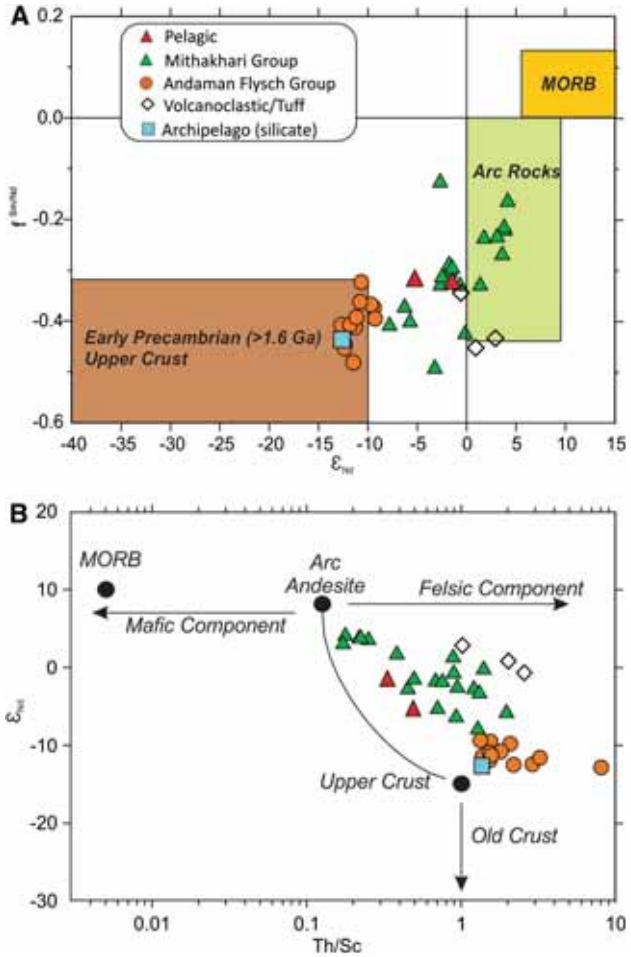

Figure 6. **(A)** f $^{Sm/Nd}$ *vs.* ε_{Nd} plot and **(B)** $\varepsilon_{Nd}(0)$ *vs.* Th/Sc plot for siliciclastics of the Andaman Accretionary Prism. Various fields and end-members are after McLennan *et al.* (1993).

because a large part of it was still an active depositional basin during the Oligocene (Licht *et al.* 2016) and the IBR, located to the west, got exhumed later in the early Miocene (Allen *et al.* 2008; Najman *et al.* 2008). Therefore, based on the overlapping isotopic compositions of Nd as well as Sr (figure 5A), albeit the lack of robustness of the latter as a provenance indicator (Awasthi *et al.* 2018), it is conceivable that either the Trans-Himalaya and the Sibumasu block located east of the west Burma block or both acted as sediment sources to the Andaman Basin during 35–20 Ma. The ε_{Nd} and $^{87}Sr/^{86}Sr$ of rocks of the Sibumasu block largely overlap with those of the Trans-Himalayan rocks (figure 5A); therefore, differentiating sediment contributions from them is difficult. However, as discussed earlier that a definite contribution from a third continental component is discernable from the observation that the sediments in the Andaman Basin became more non-radiogenic in Nd subsequent to the deposition of the Mithakhari Group (figure 3B), which suggest introduction of a new source component with $\varepsilon_{Nd}(0) < -15.0$ akin to the Higher Himalayan rocks (figure 5B) – a part of the Himalayan orogen. Sediments derived from the Higher Himalaya have been reported from the Paloegene deposits of the Assam Basin (Vadlamani *et al.* 2015), the Bengal Basin (Lindsay *et al.* 1991; Johnson and Alam 1991; Uddin and Lundberg 1998; Najman *et al.* 2008; Hossain *et al.* 2010; Roy and Roser 2013) and

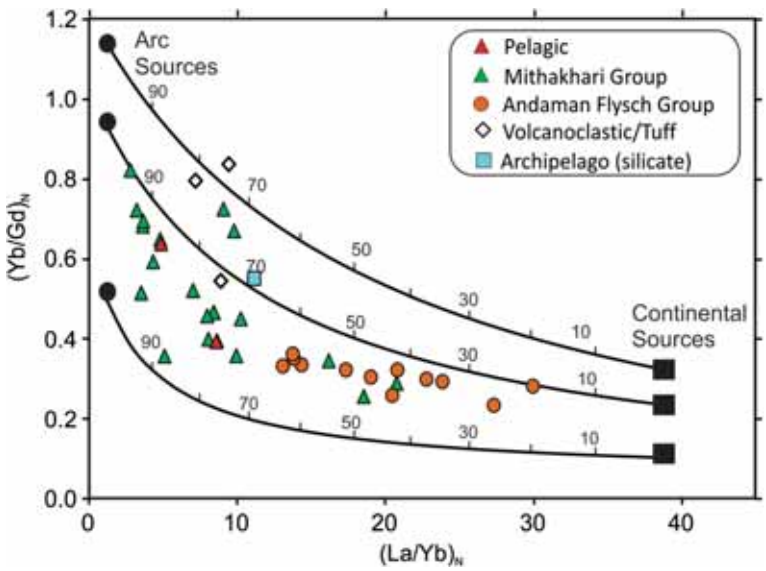

Figure 7. Chondrite normalized Yb/Gd *vs.* La/Yb plot for the Mithakhari and Andaman Flysch Group siliciclastic sediments. Binary mixing curves between three hypothetical pairs taken for continental (Himalaya) and arc (Andaman) sources are drawn to show that the Mithakhari rocks contain a large proportion of sediments derived from arc rocks, whereas the Andaman Flysch rocks contain a significant proportion of material derived from continental rocks.

the IBR (Allen *et al.* 2008), which suggest that active tectonic uplift and resulting erosion of the nascent Himalaya had already initiated during the Eocene. Therefore, it is highly likely that a part of this sediment made it to the Andaman Basin during the Oligocene.

The Sibumasu rocks having non-radiogenic $\varepsilon_{Nd}(0)$ have been observed only in the Malay Peninsula (Liew and McCulloch 1985), which is an unlikely sediment source region for the Andaman Basin because of its geographical location during the Oligocene (Hall 2012). Moreover, the southward paleocurrent directions given for the Andaman Flysch sediments (Chakraborty and Pal 2001) and proposed paleodrainage systems for Myanmar (Robinson *et al.* 2013; Lang and Huntington 2014) do not support the idea of a major sediment contribution from the Sibumasu sources, located far to the east. Some paleogeographic configuration models of the South Asian landmasses (e.g., Boonchaisuk *et al.* 2013; Huang *et al.* 2015) propose the presence of a shallow sea (Meso-Tethys) between the West Burma (magmatic arc) and Sibumasu (cratonic) terranes until Miocene time. If true, then the sediments from the Sibumasu could not have contributed significantly to the Andaman Basin, crossing the active depositional basins in the Eastern and Western Troughs on the west Burma terrane (Robinson *et al.* 2013). Therefore, we rule out contributions from the Sibumasu block as a significant reason for the compositional shifts towards non-radiogenic $\varepsilon_{Nd}(0)$ values in the basin during 35–20 Ma (figure 3B). On the other hand, the suggestion for the Himalayan provenance for these sediments is consistent with the Oligocene paleo-geographic models proposed by Hall (2012) and Replumaz *et al.* (2014).

There is no major siliciclastic unit known in the Miocene Archipelago Group (figure 2A). However, some of the carbonate turbidite formations of the group, including that exposed in the Baratang Island ($\sim$7 Ma), contain minor terrigenous sediments. The chemical and isotopic compositions of these sediments are intermediate between that of the Andaman Flysch and present-day Irrawaddy sediments, and there is a noticeable shift with time towards higher contribution from juvenile (mantle derived) sources (figure 3). There juvenile sources could have been the mid-Miocene Wuntho-Popa volcanic arc of central Myanmar (west Burma block) or the newly exhumed IBR mountains at the western margin of the Myanmar, or both, with the latter containing a significant sediment contribution from the former (Allen *et al.* 2008). The tephra from the Myanmar arc are also observed in older horizons of the group in the Havelock Island (section 4.1; figure 3). The contribution of such material to the sediment budget of the group could have been more than $\sim$70% (figure 7).

4.3 *Implications for tectonics, climate and paleodrainage*

The steady rise of the continental input to the Andaman Basin during 35–20 Ma (figure 3) is probably a result of higher erosion in the rising Tibetan–Himalayan Orogen. Although the Himalayan mountain belt and the Tibetan plateau had begun rising by $\sim$50 Ma, they attained their current elevations through multiple exhumation episodes, with the last major uplift at $\sim$10 Ma or later (An *et al.* 2001). The late Eocene ($\sim$35 Ma) change in the provenance of sediments in the Andaman Basin hints at a major tectonic activity in the orogen and a significant change in the regional climate. We believe that the high Himalayan input into the basin was a direct result of higher erosion in the mountain belts caused by higher rainfall linked to monsoon-like climatic conditions. In fact, monsoon-like conditions are believed to have prevailed in southeast Asia and China during late Eocene time (Licht *et al.* 2014; Quan *et al.* 2012, 2014).

Results of our study imply that not only the Himalayan mountain belt had attained a certain critical height during the late Eocene but also that a well-developed drainage system came into existence in the eastern India and/or in western Myanmar during this time. The latter can be considered as precursors to the modern Brahmaputra and/or Irrawaddy river systems (figure 8). These paleodrainage systems supplied sediments to the Andaman Basin and its northward extension, which would later become the IBR, from northerly and easterly sources (figure 8B). The northerly sources could have been the Trans-Himalayas and the nascent Higher-Himalaya. The question of how did these paleodrainage systems evolve remains unanswered (Curray 2005; Limonta *et al.* 2017). According to some studies, the precursors to the modern Irrawaddy had already evolved by the middle Eocene and flowed through the west Burma block (e.g., Robinson *et al.* 2013; Lang and Huntington 2014). If these channels were the only

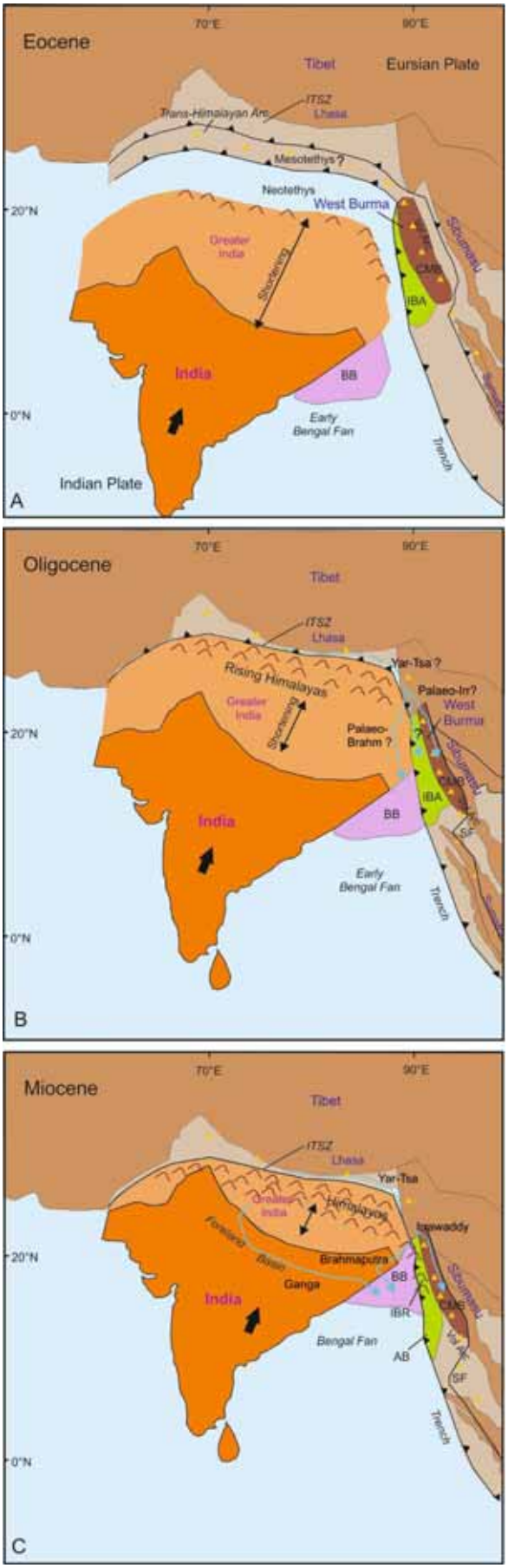

depositional pathways for sediments into the Indo–Burman–Andaman (IBA) Basin, then one would expect the Nd isotopic composition of the Oligocene sediments in the Central Myanmar Basin (CMB), deposited by the same channels, to be similar to that of the Andaman Flysch sediments. However, ε_{Nd} of CMB sediments (–8.9 to –2.4; Licht *et al.* 2016) is higher (have more radiogenic Nd) compared to the Andaman Flysch sediments (–12.7 to –9.3). In contrast, sediments of the Barail Group in the adjacent Bengal Basin, deposited by the proto-Ganga–Brahmaputra river system, have highly overlapping ε_{Nd} (–14.6 to –11.0; Hossain *et al.* 2010; Bracciali *et al.* 2015) with the latter. Therefore, it is highly likely that a proto-Ganga–Brahmaputra river system delivered sediments to the Andaman Basin too from the northwest/west (figure 8B). This also means that a significant part of the sediment budget did come from the eastern-central Himalaya. Our findings are consistent with the observations made by Limonta *et al.* (2017) based on the petrography, heavy-mineral distribution and detrital zircon geochronology in the Andaman Flysch sediments. The presence of Himalayan sediments with radiogenic Sr ($^{87}Sr/^{86}Sr > 0.715$), during 35–20 Ma, in the Andaman Basin, lends support to the proposition that a strong Himalayan input was the cause of the increase in $^{87}Sr/^{86}Sr$ of the global seawater since ∼40 Ma (Krishnaswami *et al.* 1992; Richter *et al.* 1992). The absence of deposition of pure siliciclastic formations in the Andaman Basin during 20–7 Ma makes it difficult to predict the nature of erosion in the surrounding landmasses during this period. With the development of the Irrawaddy river system, the sediment input from the IBR and the Myanmar arc increased that gradually increased the ε_{Nd} (figure 3B) leading to the composition of the sediments as observed in the modern Irrawaddy (figure 3). The modern Andaman Sea, a reconfigured version of the older trench

Figure 8. **(A–C)** A schematic of paleogeographic and tectonic evolution of South Asia during late Eocene through early Miocene as envisaged from the present study and earlier works of Hall (2012) and Morley and Searle (2017). The Greater India moved northward throughout this period with crustal shortening at its northern and eastern margins. The figure also shows plausible locations the paleo-channels of the rivers Irrawaddy (Irr), Yarlung-Tsangpo (Yar-Tsa) and Brahmaputra (Brahm), as blue arrows. BB = Bengal Basin; IBA = Indo-Burman-Andaman Basin; CMB = Central Myanmar Basin; ITSZ = Indus-Tsangpo Suture Zone; SF= Sagiang Fault; IBR = Indo-Burman Ranges; AB = Andaman Basin.

to forearc basin (Curray 2005), continues to receive IBR dominated sediments (Awasthi *et al.* 2014) delivered by the Irrawaddy river.

5. Conclusions

With the help of Sr-isotope stratigraphy and tephrochronology, we have established an improved stratigraphy for the AAP, which contains a near continuous sedimentary record of erosion of the surrounding landmasses during the Paleogene and early Neogene (55–20 Ma). Geochemical and isotopic (Sr–Nd) provenance indicators suggest that the siliciclastic sediments deposited in the Andaman Basin during most parts of the Eocene were derived primarily from the proximal Myanmar volcanic arc and contained a minor component from the continental sources in the Trans-Himalaya and/or Sibumasu block located to the east of the arc. From the late Eocene ($\sim$40 Ma) through the Oligocene there was a conspicuous change in the sediment provenance with continental crustal sources becoming the main contributors and their share increased with time, peaking at $\sim$20 Ma with $^{87}Sr/^{86}Sr$ reaching >0.73 and $\varepsilon_{Nd}(0)$ <–12.5. Paleogeographic reconstruction appears to suggest that these sources were most likely located in the nascent Himalayan mountain ranges and a paleo-Ganga–Brahmaputra river system was the main transporting agent. Such a scenario necessitates high erosion following rapid exhumation, prior to 35 Ma, in the Himalayan front under favourable monsoon-like conditions. A second major shift in provenance is recorded at $\sim$7 Ma with an increased sediment input from juvenile sources located in the IBR and Myanmar arc through a well-developed Irrawaddy river system, which continues to the present day.

Acknowledgement

We thank Alok Kumar, Bivin Geo George and Anirban Chatterjee for their help during field trips and analytical studies.

References

Allen R, Carter A, Najman Y, Bandopadhyay P C, Chapman H J, Bickle M J, Garzanti E, Vezzoli G, Ando S and Foster G L 2007 New constraints on the sedimentation and uplift history of the Andaman–Nicobar accretionary prism, South Andaman Island; *Geol. Soc. Am. Spec. Papers* **436** 223.

Allen R, Najman Y, Carter A, Barfod D, Bickle M J, Chapman H J, Garzanti E, Vezzoli G, Ando S and Parrish R R 2008 Provenance of the Tertiary sedimentary rocks of the Indo-Burman Ranges, Burma (Myanmar): Burman arc or Himalayan-derived?; *J. Geol. Soc.* **165(6)** 1045–1057.

An Z, Kutzbach J E, Prell W L and Porter S C 2001 Evolution of Asian monsoons and phased uplift of the Himalaya–Tibetan plateau since Late Miocene times; *Nature* **411(6833)** 62–66.

Awasthi N 2017 Provenance and paleo-weathering of Tertiary accretionary prism-forearc sedimentary deposits of the Andaman Archipelago, India; *J. Asian Earth Sci.* **150** 45–62.

Awasthi N, Ray E and Paul D 2018 Sr and Nd isotope compositions of alluvial sediments from the Ganga Basin and their use as potential proxies for source identification and apportionment; *Chem. Geol.* **476** 327–339.

Awasthi N, Ray J S and Pande K 2015 Origin of the Mile Tilek Tuff, South Andaman: Evidences from ^{40}Ar–^{39}Ar chronology and geochemistry; *Curr. Sci.* **108(2)** 1.

Awasthi N, Ray J S, Singh A K, Band S T and Rai V K 2014 Provenance of the Late Quaternary sediments in the Andaman Sea: Implications for monsoon variability and ocean circulation; *Geochem. Geophys. Geosyst.* **15(10)** 3890–3906.

Bandopadhyay P C and Carter A 2017 Submarine fan deposits: Petrography and geochemistry of the Andaman Flysch; *Geol. Soc. London Memoir* **47(1)** 133–140.

Bandopadhyay P C and Ghosh B 2015 Provenance analysis of the Oligocene turbidites (Andaman Flysch), South Andaman Island: A geochemical approach; *J. Earth Syst. Sci.* **124(5)** 1019–1037.

Boonchaisuk S, Siripunvaraporn W and Ogawa Y 2013 Evidence for middle Triassic to Miocene dual subduction zones beneath the Shan-Thai terrane, western Thailand from magnetotelluric data; *Gondwana Res.* **23(4)** 1607–1616.

Bracciali L, Najman Y, Parrish R R, Akhter S H and Millar I 2015 The Brahmaputra tale of tectonics and erosion: Early Miocene river capture in the Eastern Himalaya; *Earth Planet. Sci. Lett.* **415** 25–37.

Chakraborty P P and Pal T 2001 Anatomy of a forearc submarine fan: Upper Eocene–Oligocene Andaman Flysch Group, Andaman Islands, India; *Gondwana Res.* **4(3)** 477–486.

Colin C, Turpin L, Bertaux J, Desprairies A and Kissel C 1999 Erosional history of the Himalayan and Burman ranges during the last two glacial–interglacial cycles; *Earth Planet. Sci. Lett.* **171(4)** 647–660.

Curray J R 2005 Tectonics and history of the Andaman Sea region; *J. Asian Earth Sci.* **25(1)** 187–232.

Edmond J M and Huh Y 1997 *Chemical weathering yields from basement and orogenic terrains in hot and cold climates*; Tectonic uplift and climate change, Springer, pp. 329–351.

Hall R 2012 Late Jurassic–Cenozoic reconstructions of the Indonesian region and the Indian Ocean; *Tectonophys.* **570** 1–41.

Hossain H M Z, Roser B P and Kimura J I 2010 Petrography and whole-rock geochemistry of the Tertiary Sylhet succession, northeastern Bengal Basin, Bangladesh: Provenance and source area weathering; *Sedim. Geol.* **228(3)** 171–183.

Hu X, Garzanti E, Wang J, Huang W, An W and Webb A 2016 The timing of India–Asia collision onset – Facts, theories, controversies; *Earth-Sci. Rev.* **160** 264–299.

Hu X, Wang J, An W, Garzanti E and Li J 2017 Constraining the timing of the India–Asia continental collision by the sedimentary record; *Sci. China Earth Sci.* **60(4)** 603–625.

Huang W, Hinsbergen D J J, Lippert P C, Guo Z and Dupont-Nivet G 2015 Paleomagnetic tests of tectonic reconstructions of the India–Asia collision zone; *Geophys. Res. Lett.* **42(8)** 2642–2649.

Jamieson R A, Beaumont C, Medvedev S and Nguyen M H 2004 Crustal channel flows: 2. Numerical models with implications for metamorphism in the Himalayan–Tibetan orogen; *J. Geophys. Res.: Solid Earth (1978–2012)* **109(B6).**

Johnson S Y and Alam A M N 1991 Sedimentation and tectonics of the Sylhet trough, Bangladesh; *Geol. Soc. Am. Bull.* **103(11)** 1513–1527.

Kent A J R, Jacobsen B, Peate D W, Waight T E and Baker J A 2004 Isotope Dilution MC-ICP-MS Rare Earth Element Analysis of Geochemical Reference Materials NIST SRM 610, NIST SRM 612, NIST SRM 614, BHVO-2G, BHVO-2, BCR-2G, JB-2, WS-E, W-2, AGV-1 and AGV-2; *Geostand. Geoanal. Res.* **28(3)** 417–429.

Krishnaswami S, Trivedi J R, Sarin M M, Ramesh R and Sharma K K 1992 Strontium isotopes and rubidium in the Ganga–Brahmaputra river system: Weathering in the Himalaya, fluxes to the Bay of Bengal and contributions to the evolution of oceanic $^{87}Sr/^{86}Sr$; *Earth Planet. Sci. Lett.* **109(1)** 243–253.

Lang K A and Huntington K W 2014 Antecedence of the Yarlung–Siang–Brahmaputra River, eastern Himalaya; *Earth Planet. Sci. Lett.* **397** 145–158.

Lee H-Y, Chung S-L and Yang H-M 2016 Late Cenozoic volcanism in central Myanmar: Geochemical characteristics and geodynamic significance; *Lithos* **245** 174–190.

Licht A, Reisberg L, France-Lanord C, Naing Soe A and Jaeger J-J 2016 Cenozoic evolution of the central Myanmar drainage system: Insights from sediment provenance in the Minbu Sub-basin; *Basin Res.* **28(2)** 237–251.

Licht A, Van Cappelle M, Abels H A, Ladant J B, Trabucho-Alexandre J, France-Lanord C, Donnadieu Y, Vandenberghe J, Rigaudier T and Lecuyer C 2014 Asian monsoons in a late Eocene greenhouse world; *Nature* **513(7519)** 501–506.

Liew T C and McCulloch M T 1985 Genesis of granitoid batholiths of peninsular Malaysia and implications for models of crustal evolution: Evidence from a Nd–Sr isotopic and U–Pb zircon study; *Geochim. Cosmochim. Acta* **49(2)** 587–600.

Limonta M, Resentini A, Carter A, Bandopadhyay P C and Garzanti E 2017 Provenance of Oligocene Andaman sandstones (Andaman–Nicobar Islands): Ganga–Brahmaputra or Irrawaddy derived?; *Geol. Soc. London Memoir* **47(1)** 141–152.

Lindsay J F, Holliday D W and Hulbert A G 1991 Sequence Stratigraphy and the Evolution of the Ganges–Brahmaputra Delta Complex; *AAPG Bull.* **75(7)** 1233–1254.

McArthur J M, Howarth R J and Shields G A 2012 *Strontium isotope stratigraphy*; The geologic time scale **1** 127–144.

McCaffrey R 2009 The tectonic framework of the Sumatran subduction zone; *Ann. Rev. Earth Planet. Sci.* **37** 345–366.

McLennan S M, Hemming S, McDaniel D K and Hanson G N 1993 Geochemical approaches to sedimentation, provenance, and tectonics; *Special Papers – Geol. Soc. Am.* **284** 21–40.

Michard A, Gurriet P, Soudant M and Albarede F 1985 Nd isotopes in French Phanerozoic shales: External *vs.* internal aspects of crustal evolution; *Geochim. Cosmochim. Acta* **49(2)** 601–610.

Molnar P, Boos W R and Battisti D S 2010 Orographic controls on climate and paleoclimate of Asia: Thermal and mechanical roles for the Tibetan Plateau; *Ann. Rev. Earth Planet. Sci.* **38**.

Morley C K and Searle M 2017 Regional tectonics, structure and evolution of the Andaman–Nicobar Islands from ophiolite formation and obduction to collision and back-arc spreading; *Geol. Soc. London Memoir* **47(1)** 51–74.

Najman Y, Bickle M, BouDagher-Fadel M, Carter A, Garzanti E, Paul M, Wijbrans J, Willett E, Oliver G and Parrish R 2008 The Paleogene record of Himalayan erosion: Bengal Basin, Bangladesh; *Earth Planet. Sci. Lett.* **273(1)** 1–14.

Pal T, Chakraborty P P, Gupta T D and Singh C D 2003 Geodynamic evolution of the outer-arc-forearc belt in the Andaman Islands, the central part of the Burma–Java subduction complex; *Geol. Mag.* **140(03)** 289–307.

Palmer M R and Edmond J M 1992 Controls over the strontium isotope composition of river water; *Geochim. Cosmochim. Acta* **56(5)** 2099–2111.

Pedersen R B, Searle M P, Carter A and Bandopadhyay P C 2010 U–Pb zircon age of the Andaman ophiolite: Implications for the beginning of subduction beneath the Andaman–Sumatra arc; *J. Geol. Soc.* **167(6)** 1105–1112.

Pinter N and Brandon M T 1997 How erosion builds mountains; *Sci. Am.* **276(4)** 74–79.

Quan C, Liu Y-S C and Utescher T 2012 Eocene monsoon prevalence over China: A paleobotanical perspective; *Palaeogeogr. Palaeoclimatol. Palaeoecol.* **365** 302–311.

Quan C, Liu Z, Utescher T, Jin J, Shu J, Li Y and Liu Y-S C 2014 Revisiting the Paleogene climate pattern of East Asia: A synthetic review; *Earth-Sci. Rev.* **139** 213–230.

Raczek I, Jochum K P and Hofmann A W 2003 Neodymium and Strontium Isotope Data for USGS Reference Materials BCR-1, BCR-2, BHVO-1, BHVO-2, AGV-1, AGV-2, GSP-1, GSP-2 and Eight MPI-DING Reference Glasses; *Geostandards Newslett.* **27(2)** 173–179.

Rashid S A, Ahmad S, Singh S K and Absar N 2018 Elemental and Sr–Nd isotopic geochemistry of Mesoproterozoic sedimentary successions from NE Lesser Himalaya, northern India: Implications for Proterozoic climate and tectonics; *J. Asian Earth Sci.* **163** 235–248.

Ray J S, Veizer J and Davis W J 2003 C, O, Sr and Pb isotope systematics of carbonate sequences of the Vindhyan Supergroup, India: Age, diagenesis, correlations and implications for global events; *Precamb. Res.* **121(1)** 103–140.

Raymo M E and Ruddiman W F 1992 Tectonic forcing of Late Cenozoic climate; *Nature* **359** 117–122.

Replumaz A, Capitanio F A, Guillot S, Negredo A M and Villasenor A 2014 The coupling of Indian subduction and Asian continental tectonics; *Gondwana Res.* **26(2)** 608–626.

Richter F M, Rowley D B and DePaolo D J 1992 Sr isotope evolution of seawater: The role of tectonics; *Earth Planet. Sci. Lett.* **109(1)** 11–23.

Robinson R A J, Brezina C A, Parrish R R, Horstwood M S A, Oo N W, Bird M I, Thein M, Walters A S, Oliver G J H and Zaw K 2013 Large rivers and orogens: The evolution of the Yarlung Tsangpo–Irrawaddy system and the eastern Himalayan syntaxis; *Gondwana Res.* **26(1)** 112–121.

Roy D K and Roser B P 2013 Geochemical evolution of the Tertiary succession of the NW shelf, Bengal basin, Bangladesh: Implications for provenance, paleoweathering and Himalayan erosion; *J. Asian Earth Sci.* **78** 248–262.

Saha A, R Basu A, Garzione C N, Bandyopadhyay P K and Chakrabarti A 2004 Geochemical and petrological evidence for subduction-accretion processes in the Archean Eastern Indian Craton; *Earth Planet. Sci. Lett.* **220(1)** 91–106.

Sharma M, Basu A R and Ray S L 1994 Sm–Nd isotopic and geochemical study of the Archean tonalite–amphibolite association from the eastern Indian Craton; *Contrib. Mineral. Petrol.* **117(1)** 45–55.

Srinivasa Sarma D, Jafri S H, Fletcher I R and McNaughton N J 2010 Constraints on the tectonic setting of the Andaman ophiolites, Bay of Bengal, India, from SHRIMP U–Pb zircon geochronology of plagiogranite; *J. Geol.* **118(6)** 691–697.

Uddin A and Lundberg N 1998 Unroofing history of the eastern Himalaya and the Indo-Burman ranges; Heavy-mineral study of Cenozoic sediments from the Bengal Basin, Bangladesh; *J. Sedim. Res.* **68(3)** 465–472.

Vadlamani R, Wu F-Y and Ji W-Q 2015 Detrital zircon U–Pb age and Hf isotopic composition from foreland sediments of the Assam Basin, NE India: Constraints on sediment provenance and tectonics of the Eastern Himalaya; *J. Asian Earth Sci.* **111** 254–267.

Corresponding editor: Rajneesh Bhutani